Performance Considerations for General-Purpose Typing BCIs, Including the Handwriting BCI

Krishna V. Shenoy[1-3,6,7,9,10], Francis R. Willett[1,4,6,9,10], Paul Nuyujukian[1,2,4,8,9] and Jaimie M. Henderson[4-6,9]
Depts. of EE[1], BioE[2], Neurobiology[3], Neurosurgery[4], Neurology[5], NPTL[6], NPSL[7], BIL[8]
Stanford University[9] and Howard Hughes Medical Institute at Stanford University[10]
Technical Report #01, Version 2.7, 20 May 2021

Abstract[1]. This is an informal technical report regarding performance considerations for general-purpose typing brain-computer interfaces (BCIs). A general-purpose typing BCI is a BCI that enables the user to type any string of characters (as opposed to a BCI that can only type certain strings, such as sequences of words drawn from a small set of allowed words). This living document is intended to grow, evolve and serve as a resource for the community. We use our new Handwriting BCI [1] as an example system. In addition to this technical report (Technical Report #01), we are also openly sharing all electrophysiology data (Dryad, [2]) and all code (Python, GitHub, [3]) from the paper [1]. Defining and measuring performance metrics are key to our community's ability to compare, coordinate and co-operate in order to advance general-purpose typing BCIs and bring them into widespread clinical use. This report begins with investigations in people with paralysis (Sections 1-5), where our studies are part of the BrainGate2 pilot clinical trial (NCT00912041)[2] with Prof. Leigh Hochberg (sponsor-investigator), Prof. Jaimie Henderson (NPTL co-director, BrainGate2 Stanford site PI), Prof. Krishna Shenoy (NPTL co-director), Dr. Frank Willett (Research Scientist) and Prof. Paul Nuyujukian (NPTL alumnus). This report also includes pre-clinical studies with nonhuman primates (NHPs, rhesus macaques; Section 6), where our studies are part of NPSL with Prof. Krishna Shenoy (Director) and Prof. Paul Nuyujukian (NPSL alumnus). This living document is intended to be inclusive, accurate and accessible to students and investigators. We welcome suggested corrections, edits and additions; please contact Krishna Shenoy (shenoy@stanford.edu).

1 Background

In broad terms there are three main types of communication-related brain-computer interfaces (BCIs) that decode neural activity from populations of cortical neurons in order to help restore communication. These are (1) 'point-and-click cursor control' BCIs which, when operating with an on-screen keyboard, are a general-purpose typing BCI, (2) the "Brain-to-Text" attempted handwriting general-purpose typing BCI and (3) speech BCIs which decode words in conjunction with a language model with a finite dictionary size and thus, while useful in their own right, are not general-purpose typing BCIs due to the fact that only a finite set of words can be decoded (and sometimes this set is too small to restore general-purpose communication) [4–8]. These communication-related BCIs are in contrast to motor-related BCIs which stimulate arm muscles [9, 10], control robotic arms [11–13] and stimulate sensory cortices [14, 15] in order to help restore movement.

1. Point-and-click cursor control BCIs are important because they enable general-purpose computer, tablet and smart phone use without user interface modifications (i.e., neural control signals are simply provided through standard Bluetooth input protocol to the device). They enable many

[1]Please cite as: Shenoy KV, Willett FR, Nuyujukian P, Henderson JM (2021) Performance considerations for general-purpose typing BCIs, including the handwriting BCI. Technical Report #01, Version 2.7. Stanford Digital Repository (SDR), Stanford University. https://doi.org/10.25740/jx921pv3255

[2]When investigational medical devices are being tested under the permission granted by the FDA (an Investigational Device Exemption) we include, "CAUTION: Investigational Device. Limited by Federal law to investigational use."

tablet applications that we, and others, have demonstrated including web browsing, playing piano, listening to music and sending e-mails and texts by typing on an on-screen keyboard [16, 17]. Importantly, as text generation occurs by pointing at and clicking on one letter at a time, and all letters are possible, this constitutes general-purpose typing. There is no limit to the range of words possible (i.e., it has an infinite dictionary, or vocabulary, size).

However, there is an important typing speed limitation it would appear. There is a trade-off between how quickly the cursor can move (i.e., higher gain) and how well the cursor can be controlled (i.e., readily stopping on targets) [18]. This limits typing speed on an on-screen keyboard to approximately 40 correct characters per minute (ccpm) [19]. We measured typing rate with QWERTY (standard layout), OPTI-II (cursor-path minimizing layout) and alphabetical (for those unfamiliar with layouts) keyboard arrangements. We also measured achieved bitrate with a target-grid task (see Section 5) [19]. This was the highest performing general-purpose typing BCI from 2017 until 2021 ($\sim$39 ccpm [19]), when we introduced the handwriting BCI that decodes attempted handwriting ($\sim$85 ccpm) [1].

2. Given the importance of general-purpose typing BCIs, we sought a different way to increase text-generation (typing) rate. The new handwriting approach operates at the single character (letter) level, and thus has an infinitely large dictionary (i.e., open dictionary / vocabulary). Of note is that this method is also capable of typing a wide range of symbols, presumably nearly any symbols including upper case letters and characters used in other languages (e.g., Japanese Kanji), though this remains to be tested. From the paper, “We used the limited set of 31 characters shown in Fig. 1d, consisting of the 26 lower-case letters of the English alphabet, together with commas, apostrophes, question marks, full stops (written by T5 as a tilde symbol; ‘$\sim$’) and spaces (written by T5 as a greater-than symbol; >). The $\sim$ and > symbols were chosen to make full stops and spaces easier to detect. T5 attempted to write each character in print (not cursive), with each character printed on top of the previous one,” [1].

2 Typing Rate: Correct Words Per Minute

One general-purpose typing BCI performance metric that combines both typing speed and accuracy is "correct words per minute" [20]. It is defined as:

$$T = \frac{\max(S_c - S_i, 0)}{5\ t}\ \text{cwpm} \tag{1}$$

- Where T is typing rate in units of correct words per minute (cwpm)
- Where S_c is the correct number of symbols (keys) transmitted in a minute, including spaces and backspaces (deletes), in some period of time t. Note that this is also the number of total characters (correct or incorrect) minus the number of incorrect characters, in t.
- Where S_i is the incorrect number of symbols (keys) transmitted in a minute, including spaces and backspaces, in some period of time t. These incorrect symbols can be deleted with a backspace key. Note that it would appear that there is a mistaken ‘double counting’ here. But that is not the case because the incorrect characters must first be subtracted from the total number of symbols sent, and then any incorrect character must also be deleted which consumes another symbol. Thus, an incorrect symbol is appropriately counted twice.
- Where t is the measurement interval and is typically minutes to hours.

- We assume 5 characters (including spaces) per word on average as this is a typical estimate, but 6 is also sometimes used.
- Note that this cwpm measure does not leverage information-theoretic possibilities including multi-symbol channel coding (see Section 5 below and supplementary materials in [21]).

3 Typing Rate with the Handwriting BCI

As an example, let's consider the handwriting general-purpose typing BCI [1]. Its performance (i.e., text generation rate, typing rate) is as follows:

- **Characters per minute includes both correct and incorrect characters.** The average number of characters per minute (cpm) is 90 and the average character error rate is 5.4%. This appears in the paper as "Notably, typing speeds were high, plateauing at 90 characters per minute with a mean character error rate of 5.4% (averaged across all four blocks on the final day) (Fig. 2c). As there was no 'backspace' function implemented, T5 was instructed to continue writing if any decoding errors occurred," [1].
- **Correct characters per minute and correct words per minute.** Therefore 100% – 5.4% = 94.6% of the 90 cpm were correct characters. Which gives S_c = 90 cpm $\times$ 0.946 = 85.14 and S_i = 90 cpm $\times$ 0.054 = 4.86. Putting this together in Eqn. 1 yields typing rate of T = (85.14 – 4.86) / (5 $\times$ 1 minute) = **16.06 cwpm** (or 16.06 cwpm $\times$ 5 characters / word = 80.3 ccpm). If 6 characters per word is used instead 16.06 is reduced to 13.38 cwpm.
- **Comparing the performance of the two general-purpose typing BCIs.** Let's compare the handwriting general-purpose typing BCI typing rate of 16.06 cwpm with our 2D cursor point-and-click general-purpose typing BCI typing rate of 7.84 wpm (39.2 ccpm at 5 characters per word). The handwriting BCI improves performance by a factor of **16.06 cwpm** / **7.84 cwpm** = **2.05**, or simply **double** the performance. Interestingly, the same participant (T5) with the same electrode arrays (the two Utah arrays in arm/hand area of precentral gyrus) set the point-and-click typing rate record [19] three years prior to setting the new handwriting BCI typing rate record [1]. This serves as a control: array action potential signal quality is still very good, but at best it is similar to three years ago and no better. Thus this increase in performance is not attributable to more neurons or better action potential signals.
- **This performance is entirely neurally driven.** This performance relies on neural activity alone [1]. It does not use automatic spell checking and correcting, automatic word or phrase completion, or more advanced language models (machine learning natural language processing). The same is true of our point-and-click general-purpose typing BCI work [19]. These important engineering designs can be added and should further increase performance. In our point-and-click general-purpose typing BCI work with an off-the-shelf (Android) tablet computer we did use the standard Google features (e.g., word completion, word suggestion) [16].
- **Adding a language model: Performance.** We then added a large-vocabulary (50,000 word) language model as summarized in the main paper, "When a language model was used to auto-correct errors offline, error rates decreased considerably (Fig. 2c, Table 1). The character error rate decreased to 0.89% and the word error rate decreased to 3.4% averaged across all days, which is comparable to state-of-the-art speech recognition systems with word error rates of 4–5% [22, 23], putting it well within the range of usability," [1].

- **Adding a language model: Methods.** We then added a large-vocabulary (50,000 word) language model as described in detail in the paper's supplementary materials, "In a retrospective offline analysis, we used a custom, large vocabulary language model to autocorrect errors made by the decoder. Here, we give an overview of the major steps involved (note that our code release also contains the language model and associated scripts for applying it). The language model had two stages: (1) a 50,000-word bigram model that first processes the neural decoder's output to generate a set of candidate sentences, and (2) a neural network to rescore these candidate sentences (OpenAI's GPT-2, 1558M parameter version). This two-step strategy is typical in speech recognition [22] and plays to the strengths of both types of models. Although the rescoring step improved performance, we found that performance was strong with the bigram model alone (1.48% character error rate with the bigram model alone, 0.89% with rescoring, using the copy typing data). The bigram model was created with Kaldi [24] using samples of text provided by OpenAI (250,000 samples from WebText). These samples were first processed to make all text lower case and to remove all punctuation that was not part of our limited character set (consisting only of periods, question marks, commas, apostrophes, and spaces). Then, we used the Kaldi toolkit to construct a bigram language model, using the 50,000 most common words appearing in the WebText sample. The language model was represented in the form of a finite-state transducer which could be used to translate the RNN probabilities into candidate sentences [25]," [1].
- **Adding a non-causal RNN to examine limits and compare with literature.** From the paper, "Finally, to probe the limits of possible decoding performance, we trained a new RNN offline using all available sentences to process the entire sentence in a non-causal way (comparable to other BCI studies [4, 5]). Accuracy was extremely high in this regime (0.17% character error rate), indicating a high potential ceiling of performance, although this decoder would not be able to provide letter-by-letter feedback to the user." By adding sufficient latency between the time that letters (which form words and multiple-word sequences) are generated and appear on screen and the time that letters, words and multiple-word sequences are corrected a non-causal approach can be engaged in real time.

4 Performance Comparison Table

Table 1 is a survey of BCI studies that measure typing rates, achieved bitrates and information transfer rates in people with paralysis (not in people without neurological disability). Only general-purpose typing systems are included. We note that not all studies are optimized for typing rate of course; some are optimized for usability, robustness, or are not yet optimized as they are early demonstrations. Nevertheless, it is important to help provide some framework within which to start thinking about performance and how we, as a field, can advance this performance. Most of Table 1 was published in [19], and here we added the handwriting general-purpose typing BCI results [1]. Number ranges represent performance measurements across all participants for a given study.

Typing rates are readily understood to be important. Achieved bitrate is properly measured in a manner that is independent of language, which has temporal correlation structure, and independent of word completion or prediction algorithms. Similarly, information transfer rate (ITR) is also a meaningful point of comparison, though it is less reflective of practical communication rates than achieved bitrate, since achieved bitrate takes into account the need to correct errors using a simple backspace code, as detailed in [30, 39].

Study	Subjects	Rec.	Decoder	Motor impair. etiology	Avg. ccpm	Avg. cwpm	Avg. bps	Avg. ITR bps
[1] Willett et al. 2021	T5	Intra	RNN	SCI	80.30	16.06	∼6.18$^{\triangle}$	–
[26] Silversmith et al. 2020	B1	ECoG	ltCLDA	Tetraperesis	–	–	0.71	–
[19] Pandarinath*, Nuyujukian* et al. 2017	Avg (N = 3)	Intra	ReFIT-KF +HMM	ALS (2), SCI (1)	28.1	5.62	2.4	2.4
[19]	T6	"	"	ALS	31.6	6.32	2.2	2.2
[19]	T5	"	"	SCI	39.2	7.84	3.7	3.7
[19]	"	"	"	"	–	–	4.2$^{\bullet}$	4.2*
[19]	T7	"	No HMM	ALS	13.5	2.7	1.4	1.4
[27] Bacher et al. 2015	S3	Intra	CLC+LDA	BS	9.4	1.88	–	–
[28] Jarosiewicz et al. 2015	Avg (N = 4)	Intra	RTI+LDA	ALS (2), BS (2)	–	–	0.59	–
[28]	T6	"	"	ALS	"	"	0.93	–
[28]	T7	"	"	ALS	"	"	0.64	–
[28]	S3	"	"	BS	"	"	0.58	–
[28]	T2	"	"	BS	"	"	0.19	–
[29] Nijboer et al.	N = 4	EEG	P300	ALS	1.5–4.1	0.31–0.82	–	0.08–0.32
[30] Townsend et al.	N = 3	EEG	P300	ALS	–	–	0.05–0.22	–
[31] Munsinger et al.	N = 3	EEG	P300	ALS	–	–	–	0.02–0.12
[32] Mugler et al.	N = 3	EEG	P300	ALS	–	–	–	0.07–0.08
[33] Pires et al.	N = 4	EEG	P300	ALS (2), CP (2)	–	–	–	0.24–0.32
[34] Pires et al.	N = 14	EEG	P300	ALS (7), CP (5), DMD (1), SCI (1)	–	–	–	0.05–0.43
[35] Sellers et al.	N = 1	EEG	P300	BS	0.31–0.93†	0.062-0.19†	–	–
[36] McCane et al.	N = 14	EEG	P300	ALS	–	–	–	0.19
[37] Mainsah et al.	N = 10	EEG	P300-DS	ALS	–	–	–	0.01–0.60
[38] Vansteensel et al.	N = 1	ECoG	Lin. Class.	ALS	1.15‡	0.23‡	–	0.21

Table 1: Human BCI studies with highest typing rates (ccpm), typing rates (cwpm), bit rates (bps) and information transfer rates (ITR; bps). $^{\triangle}$Bit rate approximated with an empirical conversion factor 16.06 (cwpm) / 2.6 (cwpm / bps) = ∼6.18 (bps) [20]. $^{\bullet}$These numbers represent performance when measured using a denser grid (9 × 9; Fig. 3, supplemental Fig. 2 and Video 10 in [19]). $^{\beta}$For this study, reported typing rates included word prediction / completion algorithms. †Number range represents the range of performance reported for the single study participant. ‡Other reported numbers included word prediction / completion algorithms. Acronyms used: Intra – Intra-cortical; ReFIT-KF – Recalibrated Feedback Intention-Trained Kalman Filter; HMM – Hidden Markov Model; CLC – Closed-loop Calibration; LDA – Linear Discriminant Analysis; and RTI – Retrospective Target Inference. Abbreviations: Brainstem stroke (BS), Cerebral palsy (CP), Duchenne muscular dystrophy (DMD), Spinal cord injury (SCI).

5 Achieved Bitrate

Another performance metric is achieved bitrate, in units of bits per second (bps). The information throughput of the system under a single-symbol channel code – as opposed to more advanced, multi-symbol channel codes which can asymptotically approach theoretical channel capacity but are much more complex and likely not feasible for BCI users to engage in – is described in [39]. In a single-symbol channel coded keyboard, the delete key is used to correct errors one symbol or letter at a time. Achieved bit rate is defined as:

$$B = \frac{\log_2(N\text{-}1) \times \max(S_c - S_i, 0)}{t} \text{ bps} \quad (2)$$

where B is the achieved bitrate in bits per second (bps), N is the number of selectable symbols on the interface (including delete key) and the -1 is because one key is the delete key. As in Eqn. 1, S_c is the correct number of symbols, S_i is the number of incorrect symbols and t is the elapsed time. The max

Study	Decoder	Typing rate (cwpm)	Bit rate (bps)
[40] Neuralink MindPong, grid task		NHP Pager ∼2.6 × 3.67 = 9.54	3.67
[41] Kao*, Nuyujukian* et al., 2017	ReFIT-KF+HMM	NHP J ∼2.6 × 6.49 = 16.88	6.49
	ReFIT-KF+HMM	NHP R ∼2.6 × 5.71 = 14.85	5.71
	ReFIT-KF+HMM	NHP L ∼2.6 × 4.74 = 12.32	4.74
[20] Nuyujukian et al., 2017	ReFIT-KF+Dwell	NHP J 10.0	∼10.0 / 2.6 = 3.85
	ReFIT-KF+Dwell	NHP L 7.20	∼7.2 / 2.6 = 2.77
	ReFIT-KF+HMM	NHP J 12.0	∼ 12.0 / 2.6 = 4.62
	ReFIT-KF+HMM	NHP L 7.80	∼7.80 / 2.6 = 3.00
[42] Kao et al. 2015	NDF	NHP J ∼2.6 × 4.20 = 10.92	4.20
	NDF	NHP L ∼2.6 × 3.0 = 7.80	3.00
[39] Nuyujukian et al. 2015	ReFIT-KF+Dwell	NHP J ∼2.6 × 3.50 = 9.10	3.50
[39] Nuyujukian et al. 2015	ReFIT-KF+Dwell	NHP L ∼2.6 × 3.00 = 7.80	3.00
[43] Nuyujukian et al. 2014	ReFIT-FK+Dwell	NHP J ∼2.6 × 3.40 = 8.84	3.40
[43] Nuyujukian et al. 2014	ReFIT-FK+Dwell	NHP L ∼2.6 × 2.60 = 6.76	2.60

Table 2: NHP achieved typing rate (cwpm) and bit rate (bps).

function prevents bit rate from potentially being negative, which is not realistic.

Bitrate is properly measured with a grid task or another truly random sequence without correlation structure, and not with language which has such temporal correlation structure (e.g., some letters are more likely to follow the current letter than others). Thus we offer this calculation as merely an approximation – equal to what the bit rate would be if the handwriting BCI were to perform equally well on random sequences of characters selected independently with uniform probability. The handwriting BCI bit rate can be approximated in this way as:

$$\text{B} = \frac{\log_2(30) \times \max(85.14 - 4.86, 0)}{60} = \frac{4.90 \times 80.28}{60} = \textbf{6.56 bps} \quad (3)$$

Finally, let's compare this approximate handwriting general-purpose typing BCI bitrate (6.56 bps) with our point-and-click general-purpose typing BCI result (4.2 bps), which was measured with a quasi-optimal size and density grid (9 × 9 = 81 targets, Table 1, [19]). The handwriting BCI improves performance by a factor of 6.56 bps / 4.2 bps = **1.56**.

6 Performance in pre-clinical nonhuman primate (NHP) studies

We again note that not all studies are optimized for typing rate of course; some are optimized for usability, robustness, or are not yet optimized as they are early demonstrations. Nevertheless, it is important to help provide some framework within which to start thinking about performance and how we, as a field, can advance this performance. We again consider two performance metrics:

1. Typing rate in units of correct words per minute (cwpm), as described in Eqn. 1 above. This is an "effective" typing rate as NHPs clearly can't actually type letters, words and sentences with an understanding of their meaning. As a proxy, each spatial target in a grid of targets is associated with a letter in the alphabet, a backspace key for making corrections and potentially other special characters. Spatial targets are then illuminated in a sequence that corresponds to letters, from words, from sentences drawn from a corpus [20]. NHPs move a point-and-click cursor to the target and select it. If a target along the cursor's path to the requested target is accidentally selected, or if the final target selected is not the requested target, this constitutes an error.

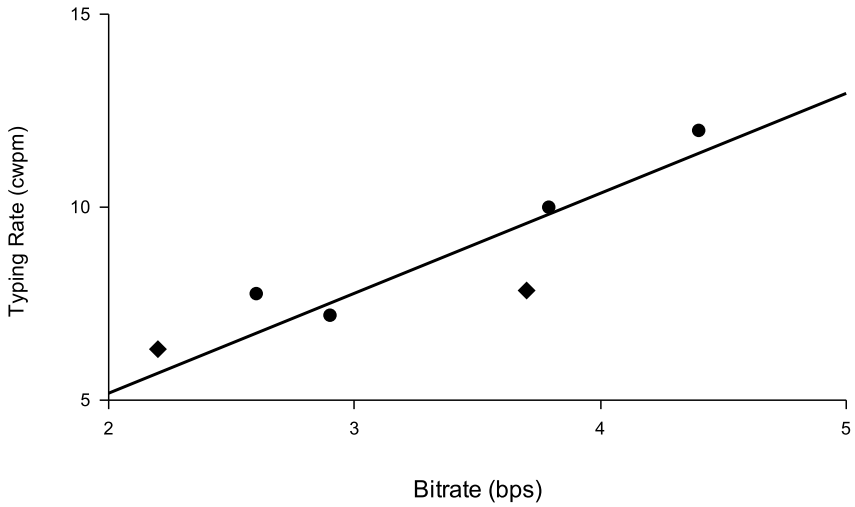

Figure 1: Typing rate vs bitrate plot on continuous cursor tasks. Circles are measurements from two NHPs [20]. Diamonds are measurements from two people in [19]. The trend line follows the equation: T (cpwm) = **2.6** Bitrate (bps).

2. Bitrate in units of bits per second (bps), as described in Eqn. 2 above. This is readily measured with a grid of targets, as targets can be illuminated in a truly random order and thus avoid temporal correlations which complicate the bitrate calculation. The relationship between typing rate (T) and bitrate (B) was estimated to be **T** = **2.6** $\times$ **B** and appears to be a reasonable approximation [20]. Note that our 2017 paper estimated the multiplier constant to convert bps to cwpm to be 2.7 [20]. Additional, recent studies in people have refined this estimate to have a multiplier constant of 2.6 which is quite similar the original estimate of 2.7 [20]. The plot deriving this new multiplier appears in Fig. 1.

Table 2 summarizes the results across recent studies. Targets were selected one of two ways. (1) A dwell time is the time that the cursor is on a target, be it the requested target or another (incorrect) target. The dwell time is optimized in order to appropriately balance between too brief a time, which leads to false clicks, and too long a time, which slows the system down [39]. (2) A 'click' signal can also be decoded from neural activity, with a click decoder operating in parallel with the cursor movement decoder (e.g., an HMM [41]). This is akin to clicking on a computer mouse's left button to select an item, and this approach generally leads to higher performance than does dwell-to-click selection.

The studies listed in Table 2 use Utah electrode arrays or Neuralink's surgical-robot (R1) insertion of

Study	Implant type	Electrodes	Implant location
[40] Neuralink Monkey MindPong	64 threads, 16 electrodes	64$\times$16 = 1,024	Contra. arm/hand PMd & M1
[41] Kao*, Nuyujukian*, et al., 2017	Utah electrode arrays	2$\times$96 = 192	Contra. arm/hand PMd & M1
[20] Nuyujukian, et al., 2017	Utah electrode arrays	2$\times$96 = 192	Contra. arm/hand PMd & M1
[44] Sussillo*,Stavisky*,Kao*,et al.,2016	Utah electrode arrays	2$\times$96 = 192	Contra. arm/hand PMd & M1
[42] Kao et al., 2015	Utah electrode arrays	2$\times$96 = 192	Contra. arm/hand PMd & M1
[39] Nuyujukian et al., 2015	Utah electrode arrays	2$\times$96 = 192	Contra. arm/hand PMd & M1
[43] Nuyujukian et al., 2014	Utah electrode arrays	2$\times$96 = 192	Contra. arm/hand PMd & M1
[45] Gilja*, Nuyujukian*, et al. 2012	Utah electrode arrays	2$\times$96 = 192	Contra. arm/hand PMd & M1

Table 3: Summary of implant technologies and locations for the studies listed in Table 2.

threads (64 threads, each with 16 electrodes along its length). Table 3 summarizes the recording technologies used in the studies listed in Table 2. It is important to note that the relationship between channel count and performance is nonlinear, with additional channels offering diminishing returns in performance [46, 47]. Additionally, each study uses different methods for channel inclusion and threshold detection and/or spike sorting. As shown in [46], when adding units in order based on a measure of informativeness, maximum performance is achieved with a subset of units. Thus, there is no simple way to normalize performance to account for implant differences.

References

1. Willett, F. R., Avansino, D. T., Hochberg, L. R., Henderson*, J. M. & Shenoy*, K. V. High-performance brain-to-text communication via handwriting. *Nature* **593,** 249–254. https://www.nature.com/articles/s41586-021-03506-2 (2021).
2. Willett, F. R., Avansino, D. T., Hochberg, L. R., Henderson*, J. M. & Shenoy*, K. V. DataDryad: All electrophysiology data reported in Willett et al. Nature 2021. *DataDryad.* https://datadryad.org/stash/dataset/doi:10.5061/dryad.wh70rxwmv (2021).
3. Willett, F. R., Avansino, D. T., Hochberg, L. R., Henderson*, J. M. & Shenoy*, K. V. GitHub: All code written and used in Willett et al. Nature 2021. *GitHub.* https://github.com/fwillett/handwritingBCI (2021).
4. Anumanchipalli, G. K., Chartier, J. & Chang, E. F. Speech synthesis from neural decoding of spoken sentences. *Nature* **568,** 493–498. http://dx.doi.org/10.1038/s41586-019-1119-1 (2019).
5. Makin, J. G., Moses, D. A. & Chang, E. F. Machine translation of cortical activity to text with an encoder-decoder framework. *Nat. Neurosci.* **23,** 575–582. http://dx.doi.org/10.1038/s41593-020-0608-8 (2020).
6. Stavisky, S. D., Willett, F. R., Wilson, G. H., Murphy, B. A., Rezaii, P., Avansino, D. T., Memberg, W. D., Miller, J. P., Kirsch, R. F., Hochberg, L. R., Ajiboye, A. B., Druckmann, S., Shenoy**, K. V. & Henderson**, J. M. Neural ensemble dynamics in dorsal motor cortex during speech in people with paralysis. *eLife* **8.** http://dx.doi.org/10.7554/eLife.46015 (2019).
7. Stavisky, S. D., Willett, F. R., Avansino, D. T., Hochberg, L. R., Shenoy**, K. V. & Henderson**, J. M. Speech-related dorsal motor cortex activity does not interfere with iBCI cursor control. *J. Neural Eng.* **17,** 016049. http://dx.doi.org/10.1088/1741-2552/ab5b72 (2020).
8. Wilson*, G. H., Stavisky*, S. D., Willett, F. R., Avansino, D. T., Kelemen, J. N., Hochberg, L. R., Henderson**, J. M., Druckmann**, S. & Shenoy**, K. V. Decoding spoken English from intracortical electrode arrays in dorsal precentral gyrus. *J. Neural Eng.* **17,** 066007. http://dx.doi.org/10.1088/1741-2552/abbfef (2020).
9. Ajiboye, A. B., Willett, F. R., Young, D. R., Memberg, W. D., Murphy, B. A., Miller, J. P., Walter, B. L., Sweet, J. A., Hoyen, H. A., Keith, M. W., Peckham, P. H., Simeral, J. D., Donoghue, J. P., Hochberg, L. R. & Kirsch, R. F. Restoration of reaching and grasping movements through brain-controlled muscle stimulation in a person with tetraplegia: a proof-of-concept demonstration. *Lancet* **389,** 1821–1830. http://dx.doi.org/10.1016/S0140-6736(17)30601-3 (2017).
10. Bouton, C. E., Shaikhouni, A., Annetta, N. V., Bockbrader, M. A., Friedenberg, D. A., Nielson, D. M., Sharma, G., Sederberg, P. B., Glenn, B. C., Mysiw, W. J., Morgan, A. G., Deogaonkar, M. & Rezai, A. R. Restoring cortical control of functional movement in a human with quadriplegia. *Nature* **533,** 247–250. http://dx.doi.org/10.1038/nature17435 (2016).
11. Hochberg, L. R., Serruya, M. D., Friehs, G. M., Mukand, J. A., Saleh, M., Caplan, A. H., Branner, A., Chen, D., Penn, R. D. & Donoghue, J. P. Neuronal ensemble control of prosthetic devices by a human with tetraplegia. *Nature* **442,** 164–171. http://dx.doi.org/10.1038/nature04970 (2006).
12. Hochberg, L. R., Bacher, D. I., Jarosiewicz, B., Masse, N. Y., Simeral, J. D., Vogel, J., Haddadin, S., Liu, J., Cash, S. S., van der Smagt, P. & Donoghue, J. P. Reach and grasp by people with tetraplegia using a neurally controlled robotic arm. *Nature* **485,** 372–375. http://dx.doi.org/10.1038/nature11076 (2012).
13. Collinger, J. L., Wodlinger, B., Downey, J. E., Wang, W., Tyler-Kabara, E. C., Weber, D. J., McMorland, A. J. C., Velliste, M. I., Boninger, M. L. & Schwartz, A. B. High-performance neuroprosthetic control by an individual with tetraplegia. *Lancet* **381,** 557–564. http://dx.doi.org/10.1016/S0140-6736(12)61816-9 (2013).
14. Flesher, S. N., Collinger, J. L., Foldes, S. T., Weiss, J. M., Downey, J. E., Tyler-Kabara, E. C., Bensmaia, S. J., Schwartz, A. B., Boninger, M. L. & Gaunt, R. A. Intracortical microstimulation of human somatosensory cortex. *Sci. Trans. Med.* **8,** 361ra141. http://dx.doi.org/10.1126/scitranslmed.aaf8083 (2016).
15. Flesher, S. N., Downey, J. E., Weiss, J. M., Hughes, C. L., Herrera, A. J., Tyler-Kabara, E. C., Boninger, M. L., Collinger, J. L. & Gaunt, R. A. Restored tactile sensation improves neuroprosthetic arm control. *Science.* https://www.biorxiv.org/content/10.1101/653428v1.abstract (2021).
16. Nuyujukian*, P., Albites Sanabria*, J., Saab*, J., Pandarinath, C., Jarosiewicz, B., Blabe, C. H., Franco, B., Mernoff, S. T., Eskandar, E. N., Simeral, J. D., Hochberg**, L. R., Shenoy**, K. V. & Henderson**, J. M. Cortical control of a tablet computer by people with paralysis. *PLoS One* **13,** e0204566. http://dx.doi.org/10.1371/journal.pone.0204566 (2018).

17. Brandman, D. M., Hosman, T., Saab, J., Burkhart, M. C., Shanahan, B. E., Ciancibello, J. G., Sarma, A. A., Milstein, D. J., Vargas-Irwin, C. E., Franco, B., Kelemen, J., Blabe, C., Murphy, B. A., Young, D. R., Willett, F. R., Pandarinath, C., Stavisky, S. D., Kirsch, R. F., Walter, B. L., Ajiboye, A. B., Cash, S. S., Eskandar, E. N., Miller, J. P., Sweet, J. A., Shenoy*, K. V., Henderson*, J. M., Jarosiewicz, B., Harrison, M. T., Simeral, J. D. & Hochberg, L. R. Rapid calibration of an intracortical brain-computer interface for people with tetraplegia. *J. Neural Eng.* **15,** 026007. http://dx.doi.org/10.1088/1741-2552/aa9ee7 (2018).

18. Willett, F. R., Young, D. R., Murphy, B. A., Memberg, W. D., Blabe, C. H., Pandarinath, C., Stavisky, S. D., Rezaii, P., Saab, J., Walter, B., Sweet, J. A., Miller, J. P., Henderson**, J. M., Shenoy**, K. V., Simeral, J. D., Jarosiewicz, B., Hochberg, L. R., Kirsch, R. F. & Ajiboye, A. B. Principled BCI decoder design and parameter selection using a feedback control model. *Scientific Reports* **9,** 8881. http://dx.doi.org/10.1038/s41598-019-44166-7 (2019).

19. Pandarinath*, C., Nuyujukian*, P., Blabe, C. H., Sorice, B. L., Saab, J., Willett, F. R., Hochberg, L. R., Shenoy**, K. V. & Henderson**, J. M. High performance communication by people with paralysis using an intracortical brain-computer interface. *eLife* **6.** http://dx.doi.org/10.7554/eLife.18554 (2017).

20. Nuyujukian, P., Kao, J. C., Ryu, S. I. & Shenoy, K. V. A nonhuman primate brain–computer typing interface. *Proc. IEEE* **105,** 66–72. http://dx.doi.org/10.1109/JPROC.2016.2586967 (2017).

21. Santhanam*, G., Ryu*, S. I., Yu, B. M., Afshar, A. & Shenoy, K. V. A high-performance brain–computer interface. *Nature* **442,** 195–198. https://doi.org/10.1038/nature04968 (2006).

22. Xiong, W., Wu, L., Alleva, F., Droppo, J., Huang, X. & Stolcke, A. The Microsoft 2017 Conversational Speech Recognition System. *arXiv.* arXiv: 1708.06073 [cs.CL]. http://arxiv.org/abs/1708.06073 (2017).

23. He, Y., Sainath, T. N., Prabhavalkar, R., McGraw, I., Alvarez, R., Zhao, D., Rybach, D., Kannan, A., Wu, Y., Pang, R., Liang, Q., Bhatia, D., Shangguan, Y., Li, B., Pundak, G., Sim, K. C., Bagby, T., Chang, S.-Y., Rao, K. & Gruenstein, A. Streaming End-to-end Speech Recognition for Mobile Devices. *Proc. IEEE Int. Conf. Acoust. Speech Signal Process (ICASSP).* http://dx.doi.org/10.1109/icassp.2019.8682336 (2019).

24. Povey, D., Ghoshal, A., Boulianne, G., Burget, L., Glembek, O., Goel, N., Hannemann, M., Motlicek, P., Qian, Y., Schwarz, P., Silovsky, J., Stemmer, G. & Vesely, K. The Kaldi speech recognition toolkit. *Proc. IEEE Workshop Autom. Speech Recognit. Underst.* https://infoscience.epfl.ch/record/192584/files/Povey_ASRU2011_2011.pdf (2011).

25. Mohri, M., Pereira, F. & Riley, M. Speech Recognition with Weighted Finite-State Transducers. *Springer Berlin Heidelberg,* 559–584 (2008).

26. Silversmith, D. B., Abiri, R., Hardy, N. F., Natraj, N., Tu-Chan, A., Chang, E. F. & Ganguly, K. Plug-and-play control of a brain–computer interface through neural map stabilization. *Nat. Biotech.* https://doi.org/10.1038/s41587-020-0662-5 (2020).

27. Bacher, D., Jarosiewicz, B., Masse, N. Y., Stavisky, S. D., Simeral, J. D., Newell, K., Oakley, E. M., Cash, S. S., Friehs, G. & Hochberg, L. R. Neural Point-and-Click Communication by a Person With Incomplete Locked-In Syndrome. *Neurorehabil. Neural Repair* **29,** 462–471. http://dx.doi.org/10.1177/1545968314554624 (2015).

28. Jarosiewicz, B., Sarma, A. A., Bacher, D., Masse, N. Y., Simeral, J. D., Sorice, B., Oakley, E. M., Blabe, C., Pandarinath, C., Gilja, V., Cash, S. S., Eskandar, E. N., Friehs, G., Henderson**, J. M., Shenoy**, K. V., Donoghue, J. P. & Hochberg, L. R. Virtual typing by people with tetraplegia using a self-calibrating intracortical brain-computer interface. *Sci. Trans. Med.* **7,** 313ra179. http://dx.doi.org/10.1126/scitranslmed.aac7328 (2015).

29. Nijboer, F., Sellers, E. W., Mellinger, J., Jordan, M. A., Matuz, T., Furdea, A., Halder, S., Mochty, U., Krusienski, D. J., Vaughan, T. M., Wolpaw, J. R., Birbaumer, N. & Kübler, A. A P300-based brain–computer interface for people with amyotrophic lateral sclerosis. *Clin. Neurophysiol.* **119,** 1909–1916. https://www.sciencedirect.com/science/article/pii/S1388245708002393 (2008).

30. Townsend, G., LaPallo, B. K., Boulay, C. B., Krusienski, D. J., Frye, G. E., Hauser, C. K., Schwartz, N. E., Vaughan, T. M., Wolpaw, J. R. & Sellers, E. W. A novel P300-based brain–computer interface stimulus presentation paradigm: Moving beyond rows and columns. *Clin. Neurophysiol.* **121,** 1109–1120. https://www.sciencedirect.com/science/article/pii/S1388245710000738 (2010).

31. MünSSinger, J. I., Halder, S., Kleih, S. C., Furdea, A., Raco, V., Hösle, A. & Kübler, A. Brain Painting: First evaluation of a new brain-computer interface application with ALS-patients and healthy volunteers. *Frontiers in Neuroscience* **4,** 182. http://journal.frontiersin.org/article/10.3389/fnins.2010.00182/abstract (2010).

32. Mugler, E. M., Ruf, C. A., Halder, S., Bensch, M. & Kubler, A. Design and implementation of a P300-based brain-computer interface for controlling an internet browser. *IEEE Trans. Neural Sys. Rehab. Eng.* **18,** 599–609. http://dx.doi.org/10.1109/TNSRE.2010.2068059 (2010).

33. Pires, G., Nunes, U. & Castelo-Branco, M. Statistical spatial filtering for a P300-based BCI: tests in able-bodied, and patients with cerebral palsy and amyotrophic lateral sclerosis. *Journal of Neuroscience Methods* **195,** 270–281. http://dx.doi.org/10.1016/j.jneumeth.2010.11.016 (2011).

34. Pires, G., Nunes, U. & Castelo-Branco, M. Comparison of a row-column speller vs. a novel lateral single-character speller: assessment of BCI for severe motor disabled patients. *Clin. Neurophysiol.* **123,** 1168–1181. http://dx.doi.org/10.1016/j.clinph.2011.10.040 (2012).

35. Sellers, E. W., Ryan, D. B. & Hauser, C. K. Noninvasive brain-computer interface enables communication after brainstem stroke. *Sci. Trans. Med.* **6,** 257re7. http://dx.doi.org/10.1126/scitranslmed.3007801 (2014).

36. McCane, L. M., Heckman, S. M., McFarland, D. J., Townsend, G., Mak, J. N., Sellers, E. W., Zeitlin, D., Tenteromano, L. M., Wolpaw, J. R. & Vaughan, T. M. P300-based brain-computer interface (BCI) event-related potentials (ERPs): People with amyotrophic lateral sclerosis (ALS) vs. age-matched controls. *Clin. Neurophysiol.* **126,** 2124–2131. http://dx.doi.org/10.1016/j.clinph.2015.01.013 (2015).

37. Mainsah, B. O., Collins, L. M., Colwell, K. A., Sellers, E. W., Ryan, D. B., Caves, K. & Throckmorton, C. S. Increasing BCI communication rates with dynamic stopping towards more practical use: an ALS study. *J. Neural Eng.* **12,** 016013. http://dx.doi.org/10.1088/1741-2560/12/1/016013 (2015).

38. Vansteensel, M. J., Pels, E. G. M., Bleichner, M. G., Branco, M. P., Denison, T., Freudenburg, Z. V., Gosselaar, P., Leinders, S., Ottens, T. H., Van Den Boom, M. A., Van Rijen, P. C., Aarnoutse, E. J. & Ramsey, N. F. Fully Implanted Brain-Computer Interface in a Locked-In Patient with ALS. *New England J. Med.* **375,** 2060–2066. http://dx.doi.org/10.1056/NEJMoa1608085 (2016).

39. Nuyujukian, P., Fan, J. M., Kao, J. C., Ryu, S. I. & Shenoy, K. V. A high-performance keyboard neural prosthesis enabled by task optimization. *IEEE Trans. Biomed. Eng.* **62,** 21–29. http://dx.doi.org/10.1109/TBME.2014.2354697 (2015).

40. Neuralink. Neuralink Monkey MindPong: Pong and Grid Task. *Neuralink Blog*. https://neuralink.com/blog/ (2021).

41. Kao, J. C., Nuyujukian, P., Ryu, S. I. & Shenoy, K. V. A high-performance neural prosthesis incorporating discrete state selection with hidden Markov models. *IEEE Trans. Biomed. Eng.* **64,** 935–945. http://dx.doi.org/10.1109/TBME.2016.2582691 (2017).

42. Kao, J. C., Nuyujukian, P., Ryu, S. I., Churchland, M. M., Cunningham, J. P. & Shenoy, K. V. Single-trial dynamics of motor cortex and their applications to brain-machine interfaces. *Nature Communications* **6,** 7759. http://dx.doi.org/10.1038/ncomms8759 (2015).

43. Nuyujukian, P., Kao, J. C., Fan, J. M., Stavisky, S. D., Ryu, S. I. & Shenoy, K. V. Performance sustaining intracortical neural prostheses. *J. Neural Eng.* **11,** 066003. http://dx.doi.org/10.1088/1741-2560/11/6/066003 (2014).

44. Sussillo*, D., Stavisky*, S. D., Kao*, J. C., Ryu, S. I. & Shenoy, K. V. Making brain-machine interfaces robust to future neural variability. *Nat. Comm.* **7,** 13749 (2016).

45. Gilja, V., Nuyujukian, P., Chestek, C. A., Cunningham, J. P., Yu, B. M., Fan, J. M., Churchland, M. M., Kaufman, M. T., Kao, J. C., Ryu, S. I. & Shenoy, K. V. A high-performance neural prosthesis enabled by control algorithm design. *Nat. Neurosci.* **15,** 1752–1757. http://dx.doi.org/10.1038/nn.3265 (2012).

46. Sanchez, J. C., Carmena, J. M., Lebedev, M. A., Nicolelis, M. A. L., Harris, J. G. & Principe, J. C. Ascertaining the importance of neurons to develop better brain-machine interfaces. *IEEE Trans. Biomed. Eng.* **51,** 943–953. http://dx.doi.org/10.1109/TBME.2004.827061 (2004).

47. Wahnoun, R., He, J. & Helms Tillery, S. I. Selection and parameterization of cortical neurons for neuroprosthetic control. *J. Neural Eng.* **3,** 162–171. http://dx.doi.org/10.1088/1741-2560/3/2/010 (2006).